process is possible it seems reasonable that quenching in all three cases occurs by a similar mechanism. The consistent fall-off in quenching over the series 4S6A, S10A, and S12A with all three quenchers supports a picture in which the distance dependence indicated by the extended structure of the stilbene-polymethylenecarboxylic acid is maintained in the supported multilayers. Whether the actual distances between stilbene edge and the hydrophilic acceptor is as great as indicated above could be questioned. Some possibilities for reducing this could include "roughness" of the hydrophilic interface which could be due to interdigitation or other phenomena. Though this could reduce the distance it would not alter the changes in distance as the different stilbenes are compared. The observation of rapid electron transfer over what appears to be relatively long distances in the assemblies is consistent with rate/distance relationships measured in other recent studies.[29-32,34] This similarity suggests that tunneling mechanisms developed for frozen solutions or hydrocarbon "spacer" probably apply equally well for these Langmuir-Blodgett assemblies.[10-14] The hydrophobic and interchanin stilbenes have thus been demonstrated as useful chromophores for incorporation in assemblies to investigate phenomena occurring at distances greater than contact/collisional but shorter than the span of two fatty acid chains. Their predilection for formation of H aggregates is an interesting but in some ways unfortunate characteristic which limits their use in an antenna or energy harvesting function; however, the features of these aggregates which make them ineffective as light harvesting pigments (low extinction coefficient, short wavelength absorption, and inefficient energy donation) could make them useful as energy receptors in future investigations.

Acknowledgment. We thank the National Science Foundation (Grants CHE-8121140 and CHe-8315303) for support of this work. We also thank Marjorie Richter for her technical assistance and patience in preparing films and supported multilayers.

Registry No. 4S6A, 91202-35-6; S10A, 77824-98-7; S12A, 77814-49-4; Co18, 103439-09-4; Co218, 103439-10-7; V218, 64055-17-0; T218, 29523-00-0; *trans*-$[Co(en)_2Br_2]Br$, 15005-14-8; arachidic acid, 506-30-9; palmitic acid, 57-10-3.

Model for the Structure of the Liquid Water Network[1]

Ernest Grunwald

Contribution from the Chemistry Department, Brandeis University, Waltham, Massachusetts 02254. *Received February 18, 1986*

Abstract: The state of a water molecule in liquid water is defined by its time-average network environment. Two states are characterized. State A is the familiar four-coordinated state of the Bernal-Fowler model with tetrahedral hydrogen bonds. State B is five-coordinated. Reexamination of the static dielectric constant by the method of Oster and Kirkwood confirms the marked polar character of the four-coordinated state but shows that the five-coordinated state is only about half as polar. Explicit five-coordinated models are proposed which are consistent with polarity and satisfy constraints of symmetry and hydrogen-bond stoichiometry. The potential energy due to the dipole-dipole interaction of the central water molecule with its time-average solvent network is derived without additional parameters. This permits prediction of barriers to rotation, frequencies for hindered rotation and libration in the network, and $\Delta H_{A,B}$ and $\Delta S_{A,B}$. The results are in substantial agreement with relevant experiments. In particular, the barriers to rotation permit a consistent interpretation of the dielectric relaxation spectrum. The relative importance of the two states varies predictably with the property being examined, and this can account for some of the "schizophrenia" of aqueous properties. Since the two-state model is based on time-average network configurations, it does not apply when the time scale of observation is short compared to network frequencies, i.e., at infrared frequencies where continuum models may be successful.

In recent years there has been marked progress in computer simulations of liquid water and of aqueous solutions.[2-5] These studies use the deductive scientific approach: They begin with a model and reason to the facts. The present paper tries to characterize the structure of the liquid water network by using the alternative inductive approach, beginning with facts and reasoning to a model.

The resulting model will be consistent with the free energy and its temperature derivatives, the dielectric constant, the probable number of hydrogen-bonded nearest neighbors, intermolecular vibration frequencies, and dielectric relaxation dynamics. The model is explicit enough to be useful for prediction. In particular, it can explain the peculiar pattern of thermodynamic properties of nonpolar solutes in water which is commonly called "hydrophobic hydration".[6,7] This application of the model will be reported separately.[8]

A key issue which any model of liquid water should face is the striking resemblance of the properties of water to those of a mixture consisting of two states in equilibrium.[9-13] One state, call it state A, has a relatively low energy, low entropy, and large

(1) Work supported in part by a grant from the National Science Foundation.

(2) (a) Stillinger, F. H.; Rahman, A. *J. Chem. Phys.* **1974**, *60*, 1545; **1978**, *68*, 666. (b) Stillinger, F. H. *Science (Washington, D.C.)* **1980**, *209*, 451.

(3) (a) Hodes, Z. I.; Nemethy, G.; Scheraga, H. A. *Biopolymers* **1979**, *18*, 1565. (b) Rossky, P. J.; Karplus, M. *J. Am. Chem. Soc.* **1979**, *101*, 1913. (c) Linse, P.; Karlstrom, G.; Jonsson, B. *J. Am. Chem. Soc.* **1984**, *106*, 4097. (d) Rosenberg, R. O.; Berne, B. J.; Chandler, D. *Chem. Phys. Lett.* **1980**, *75*, 162. (e) Clementi, E. *J. Phys. Chem.* **1985**, *89*, 4426. (f) Rossky, P. J.; Hirata, F. In *Molecular-Based Study of Fluids*; Haile, J. M., Mansoori, G. A., Eds.; Advances in Chemistry 204; American Chemical Society: Washington, DC, **1983**, p 281.

(4) (a) Jorgensen, W. L.; Chandrasekhar, J.; Madura, J. D.; Impey, R. W.; Klein, M. L. *J. Chem. Phys.* **1983**, *79*, 926. (b) Jorgensen, W. L. *J. Chem. Phys.* **1982**, *77*, 5757; *J. Phys. Chem.* **1983**, *87*, 5304.

(5) (a) Mehrotra, P. K.; Beveridge, D. L. *J. Am. Chem. Soc.* **1980**, *102*, 4287. (b) Marchese, F. T.; Beveridge, D. L. *J. Am. Chem. Soc.* **1984**, *106*, 3713. (c) Ravishanker, G.; Mehrotra, P. K.; Mezei, M.; Beveridge, D. L. *J. Am. Chem. Soc.* **1984**, *106*, 4102. (d) Beveridge, D. L.; Mezei, M.; Mehrotra, P. K.; Marchese, M. T.; Ravi-Shanker, G.; Vasu, T.; Swaminathan, S. *Molecular-Based Study of Fluids*; Haile, J. M., Mansoori, G. A., Eds.; Advnces in Chemistry 204; American Chemical Society: Washington, DC, 1983; p 297.

(6) (a) Ben-Naim, A. *Hydrophobic Interactions*; Plenum Press: New York, 1980. (b) Tanford, C. *The Hydrophobic Effect. Formation of Micelles and Biological Membranes*, 2nd ed.; Wiley: New York, 1980. (c) Lumry, R.; Battistel, E.; Jolicoeur, C. *Faraday Symp. Chem. Soc.* **1982**, *17*, 93.

(7) (a) Franks, F. In *Water, A Comprehensive Treatise*; Franks, F.; Ed.; Plenum Press: New York, 1975; Vol. 4, Chapter 1. (b) Chan, D. Y. C.; Mitchell, D. J.; Ninhum, B. W.; Pailthorpe, B. A. *Ibid.*; 1979; Vol. 6, Chapter 5.

(8) Grunwald, E. *J. Am. Chem. Soc.*, following paper in this issue.

(9) Benson, S. W. *J. Am. Chem. Soc.* **1978**, *100*, 5640.

(10) Angell, C. A. *J. Phys. Chem.* **1971**, *75*, 3698.

0002-7863/86/1508-5719$01.50/0

volume. The other state, B, has a relatively high energy, high entropy, and small volume. The hypothesis of two states in equilibrium is consistent with properties of liquid water ranging from its thermodynamic properties[9,10] to its infrared[11,12] and Raman[13] spectrum. The two-state model has never been embraced unreservedly by theoreticians, and in fact one can usually suggest a plausible alternative, for instance, a continuum of states for infrared spectra[14,15] or five discrete states for thermodynamic properties.[16] It is significant, therefore, that experimentalists, even those with theoretical misgivings, so often return to the two-state model in order to rationalize their data.[17a]

When the two-state approach is applied to spectral properties, one finds from the temperature dependence of the absorbances that the mass action expression is that for an one-to-one equilibrium: $RT^2\, d\ln([B]/[A])/dT = \Delta H_{A,B}$.[11-13] Thus the interconversion of the two states is an isomerization of, or within, the water network, rather than a process in which the polymeric network dissociates into two or more translationally independent units.

During the 1950s and 1960s, when hydrogen bonds among water molecules were thought to have directional properties like those of covalent bonds,[18] it was reasonable to regard the low-energy–low-entropy state A as consisting of network bonds that are directional, icelike hydrogen bonds.[10-13] In the second state, B, the network bonds were thought to be broken, or energized, to a condition of greater flexibility.[10-13] The relatively large volume of state A was associated with its icelike character.[9,10] According to some views, state A consisted of, or included, well-ordered clathrate-like complexes of water molecules.[12,19]

This interpretation may not be tenable today. Ab initio quantum-mechanical calculations for hydrogen-bonded water dimers and trimers[20,21] indicate that the potential surfaces are rather flat for bending and rocking motions about the hydrogen bond and for internal rotations about the hydrogen-bond axis. In particular, they do not show any obvious features that might describe a distinctive subspecies of low energy and low entropy. As a result, it is unlikely that the two states are subspecies associated with individual hydrogen bonds. More likely, they represent two kinds of nearest-neighbor shells around a water molecule.

Plan. In the present model, the two states are assigned to two different kinds of nearest-neighbor shells with flexible hydrogen bonds, surrounding an otherwise constant central water molecule. One of the states is the familiar four-coordinated state of the Bernal–Fowler model,[22] with tetrahedrally oriented hydrogen bonds. The other state is outside the Bernal–Fowler framework.

The model is developed from the following properties. 1. The heat capacity of liquid water is used to obtain a set of two-state parameters $\Delta H_{A,B}$ and $\Delta S_{A,B}$, as described by Benson.[9] 2. The mean number of hydrogen-bonded nearest neighbors, inferred from the experimental oxygen–oxygen radial distribution function,[23,24] then indicates that the second state is five-coordinated. 3. Following Oster and Kirkwood,[25] the static dielectric constant $\epsilon(T)$ is used to evaluate the polar character of the two states. The highly polar tetrahedral character of the four-coordinated state is confirmed. The five-coordinated state is found to be only half as polar.

These results are then developed into an explicit model, as follows. 1. Time-average hydrogen-bonded network structures are deduced for the five-coordinated state by the method of Oster and Kirkwood,[25a] subject to constraints of symmetry and hydrogen-bonding stoichiometry. 2. Expressions are derived for the dipole–dipole interactions and barriers to rotation in both states. 3. The potential functions obtained in 2 are used to calculate quantum levels and oscillator frequencies for hindered rotation and libration of a water molecule in its network site, as well as $\Delta S_{A,B}$ and $\Delta H_{A,B}$, which are then compared with experimental parameters. 4. The relatively low barrier predicted for hindered rotation in the five-coordinated state is confirmed by kinetic analysis of dielectric relaxation.

Relevance to Computer Simulations. An attractive feature of the computer simulation of a liquid is that the model is stark and visible, being expressed by an equation, the intermolecular potential. A weakness is that the path from model to simulated results, involving millions of computations, is so long and tortuous that one loses sight of the individual steps. Thus, if the model must be improved, the computations provide no clear clues as to which parts of the model must be changed. It is for this reason that inductive methods retain their usefulness, because they are efficient at defining the qualitative features that a valid model must possess.

According to recent reviews,[3e,4,5d] the potential functions that have been used in simulations of liquid water by molecular dynamics or Monte Carlo methods all try to describe the Bernal–Fowler model.[22] For instance, the original potential of Stillinger and Ben-Naim[26]—an effective pairwise potential—assumes that each water molecule interacts with the surrounding molecules cumulatively by two separate interactions: a short-range Lennard–Jones interaction and a long-range electrostatic interaction in which the water dipole is treated as a set of two positive and two negative point charges which represent respectively the hydrogen bond donor and acceptor affinities of the water molecule.[2] This potential, and others of similar genre,[4a,5d] fit some properties of water well but fail to fit others. Two failures will be mentioned. First, the simulated oxygen–oxygen radial distribution functions, while reproducing the 2.9-Å peak due to hydrogen-bonded nearest neighbors and the 4.8-Å peak due to next-nearest neighbors on a tetrahedral Bernal–Fowler lattice, fail to show the peak near 3.7 Å whose real existence is well established by Narten and Levy's X-ray diffraction data.[23] It may be significant that the five-coordinated state in the present model is outside the Bernal–Fowler framework. Second, as elucidated in a recent review,[3f] the computer simulations do not yield well-defined frequencies for intermolecular vibrations in the water network, contrary to observation.[13b]

Thermodynamic Data for Two-State Model. As stated previously, the equilibrium between states A and B conforms to an 1:1 mass-action expression. Let α denote the fraction of water

(11) (a) Worley, J. D.; Klotz, I. M. *J. Chem. Phys.* **1966**, *45*, 2868. (b) Senior, W. A.; Verrall, R. E. *J. Phys. Chem.* **1969**, *73*, 4242.

(12) For reviews of mixture models, see: (a) Davis, C. M.; Jarzynski, J. In *Water and Aqueous Solutions. Structure, Thermodynamics and Transport Properties*; Horne, R. A., Ed.; Wiley-Interscience: New York, 1972; Chapter 10. (b) Eisenberg, D.; Kauzmann, W. *The Structure and Properties of Water*; Oxford University Press: New York, 1969. (c) Reference 6a.

(13) (a) Walrafen, G. E. *J. Chem. Phys.* **1964**, *40*, 3249. (b) *Ibid.* **1967**, *47*, 114. (c) *Ibid.* **1968**, *48*, 244.

(14) (a) Wall, T. T.; Hornig, D. F. *J. Chem. Phys.* **1965**, *43*, 2079. (b) Schiffer, J.; Hornig, D. F. *Ibid.* **1968**, *49*, 4150.

(15) (a) Falk, M.; Ford, T. A. *Can. J. Chem.* **1966**, *44*, 1699. (b) Ford, T. A.; Falk, M. *Ibid.* **1968**, *46*, 3579. (c) Luck, W. A. P.; Ditter, W. *J. Phys. Chem.* **1970**, *74*, 3687.

(16) Nemethy, G.; Scheraga, H. A. *J. Chem. Phys.* **1962**, *36*, 3382; **1964**, *41*, 680.

(17) (a) For a review of other models, see: Cogley, D. R.; Falk, M.; Butler, J. N.; Grunwald, E. *J. Phys. Chem.* **1972**, *76*, 855. (b) Litovitz, T.; Carnevale, E. *J. Appl. Phys.* **1955**, *26*, 816.

(18) Pimentel, G. C.; McClellan, A. L. *The Hydrogen Bond*; W. H. Freeman and Co.: San Francisco, 1960.

(19) For reviews, see: (a) Frank, H. S. In *Water, A Comprehensive Treatise*; Franks, F., Ed.; Plenum Press: New York, 1972; Vol. 1, p 539. (b) Davidson, D. W. *Ibid.* **1973**; Vol. 2, Chapter 3.

(20) Del Bene, J.; Pople, J. A. *J. Chem. Phys.* **1970**, *52*, 4858.

(21) Hankins, D.; Moskowitz, J. W.; Stillinger, F. H. *J. Chem. Phys.* **1970**, *53*, 4544.

(22) Bernal, S. D.; Fowler, R. H. *J. Chem. Phys.* **1933**, *1*, 515.

(23) (a) Narten, A. H.; Levy, H. A. *J. Chem. Phys.* **1971**, *55*, 2263. (b) *Ibid. Science (Washington, D.C.)* **1969**, *165*, 447. This article gives large-scale plots of experimental distribution functions. (c) Narten, A. H.; Thiessen, W. E.; Blum, L. *Science (Washington, D.C.)* **1982**, *217*, 1033 (neutron diffraction).

(24) (a) Morgan, J.; Warren, B. E. *J. Chem. Phys.* **1938**, *6*, 666. (b) Brady, G. W.; Romanow, W. J. *J. Chem. Phys.* **1960**, *32*, 306.

(25) (a) Oster, G.; Kirkwood, J. G. *J. Chem. Phys.* **1943**, *11*, 175. (b) Kirkwood, J. G. *J. Chem. Phys.* **1939**, *7*, 911; *Trans. Faraday Soc.* **1946**, *42A*, 7.

(26) (a) Ben-Naim, A.; Stillinger, F. H. *Water, Aqueous Solutions*; Structure, *Thermodynamics, Transport Processes*; Horne, R. A., Ed.; Interscience: New York, 1972; pp 295–330. (b) Ben-Naim, A. *Water and Aqueous Solutions. Introduction to a Molecular Theory*; Plenum: New York, 1974.

Table I. Some Data for Two-State Model of Water

T, °C	α^a	$\langle m \rangle^b$	g^c	$\alpha_{dip}{}^d$
0	0.769	4.23	2.75	0.70
25	0.694	4.31	2.68	0.63
62	0.587	4.41	2.56	0.54
83	0.532	4.47	2.49	0.50

[a] Equation 1: $\Delta H_{A,B} = 2.5_1$ kcal/mol; $\Delta S_{A,B} = 6.7_5$ cal/mol K. [b] Equation 2: $m_A = 4$; $m_B = 5$. [c] Kirkwood correlation factor, eq 4. Data from ref 25a. [d] Predicted on the basis of dipole potential, eq 14, and eq 1. $\Delta H_{A,B} = 2.0_2$ kcal/mol; $\Delta S_{A,B} = 5.6_8$ cal/mol K.

molecules in state A. The statewise equilibrium constant then is defined in (1a) and the related thermodynamic parameters in (1b).

$$(1 - \alpha)/\alpha = K \tag{1a}$$

$$-RT \ln K = \Delta G_{A,B} = \Delta H_{A,B} - T\Delta S_{A,B} \tag{1b}$$

Of the various sets of $\alpha(T)$ that have been recommended,[12] the present model will use the "internally consistent set" ($\Delta H_{A,B} = 2.5_1$ kcal/mol, $\Delta S_{A,B} = 6.7_5$ cal/(mol K)) obtained by Benson[9] from an analysis of the heat capacity of water. This set was chosen because (1) $\Delta H_{A,B}$ and $\Delta S_{A,B}$ (whose accuracy is important in this work) are obtained directly rather than indirectly from the effect of temperature on α; (2) the 2.5 kcal/mol value of $\Delta H_{A,B}$ agrees with values based on infrared (2.4, 2.3)[11] and Raman (2.5)[13] spectra; and (3) although Raman and IR results[11,13] do not give values for $\Delta S_{A,B}$, they do show that $\Delta H_{A,B}$ is approximately constant in the normal liquid range. Benson's assumption[9] that $\Delta H_{A,B}$ and $\Delta S_{A,B}$ are independent of the temperature is therefore consistent with independent evidence.

On the other hand, the part of Benson's treatment[9] which deals with molar volumes (v) will be omitted because it is likely, from the temperature dependence of the 3.7-Å peak in the oxygen–oxygen radial distribution function,[23b] that $\Delta v_{A,B}$ varies with temperature.

The thermodynamic parameters due to Angell,[10] which the author has used previously,[27a] will not be used now because they assume that the two states are states of the individual hydrogen bonds rather than of the nearest-neighbor shells around the water molecules and thus are not consistent with the present model.

Values of α at representative temperatures have been computed from eq 1 and are listed in Table I.

Coordination Numbers. By definition, the coordination number of a water molecule in the liquid network is equal to the number of hydrogen-bonded nearest neighbors. In principle, the mean coordination number $\langle m \rangle$ for the liquid can be deduced from the area of the 2.9-Å nearest-neighbor peak in the oxygen–oxygen radial distribution function. In their pioneering X-ray diffraction work, Morgan and Warren[24a] obtained values of $\langle m \rangle$ ranging from 4.4 at 0 °C to 4.9 at 83 °C. More recently, Narten and Levy,[23] in a thorough reinvestigation, found $\langle m \rangle$ to be rather insensitive to temperature and obtained a value of 4.4 at 25 °C.[23b] They also stated that all values reported for $\langle m \rangle$ at present are approximate because of assumptions required in the calculations. In particular, the values reported by Morgan and Warren[24a] probably represent upper limits because of imperfect deconvolution of the 3.7-Å peak. This problem becomes accentuated above 60 °C.

In terms of the two-state model, $\langle m \rangle$ is given by eq 2. It is

$$\langle m \rangle = \alpha m_A + (1 - \alpha) m_B \tag{2}$$

widely agreed[13a] that the icelike low-energy and low-entropy state A has $m_A = 4$, as envisaged by the Bernal–Fowler model[22] and supported by the Oster–Kirkwood interpretation of the dielectric constant.[25a] Since the mean value $\langle m \rangle$ for the overall liquid is greater than 4, m_B is an integer greater than 4. As shown in Table I, on letting $m_A = 4$ and $m_B = 5$, one can compute values of $\langle m \rangle$ from (2) that range from 4.23 at 0 °C to 4.47 at 83 °C, in substantial agreement with the X-ray results. If Narten and Levy had not warned against overinterpretation, one might consider the matter as settled. The choice of $m_B = 6$, while physically possible, is statistically improbable, and values of $m_B > 6$ are ruled out by the data. Since the set $m_A = 4$, $m_B = 5$ is also compatible with other properties of liquid water, it will be used throughout this paper.

Dipole Moments. Interpretation of the dielectric constant in terms of Kirkwood's theory[25b] gives information about the electric dipole moment of the solvent network surrounding a water molecule. One can deduce the component of the average dipole moment along an axis parallel to the dipole moment of the central water molecule. By analyzing this property in terms of the two-state model, one can then evaluate the polar character of the two network states.

The following treatment is based on Oster and Kirkwood's (OK) original paper.[25a] The key equations are (3)–(5). Here ϵ denotes

$$(\epsilon - 1)(2\epsilon + 1)/9\epsilon = (4\pi N/3v)(\chi + g\mu^2/3kT) \tag{3}$$

$$(g - 1)\mu^2 = \mu \cdot \langle \mu_{nwrk} \rangle \tag{4}$$

$$g - 1 = \alpha(g_A - 1) + (1 - \alpha)(g_B - 1) \tag{5}$$

the static dielectric constant at temperature T, v is the molar volume, N is Avogadro's number, χ is the molecular polarizability, μ is the dipole moment of the central water molecule, and $\langle \mu_{nwrk} \rangle$ is the ensemble-average dipole moment of the surrounding solvent network. Equation 4 relates the dipole correlation factor g, defined by Kirkwood,[25b] to the scalar product of $\mu \cdot \langle \mu_{nwrk} \rangle$. Equation 5 expresses g in terms of g_A, g_B, and the state fractions. In principle, g_A and g_B are functions of α. The following will show, however, that the variations are slight compared to experimental errors, so that g_A and g_B may be treated as constants.

Values of g as calculated by OK[25a] from the dielectric constant of water are listed in Table I. OK showed that the values are in solid agreement with a tetrahedral network environment but pointed out two inconsistencies in their analysis. First, the coordination number used by them was greater than 4—they actually used values ranging from 4.4 to 4.9 as reported by Morgan and Warren.[24a] Second, g as derived from the dielectric data (Table I) decreases significantly with increasing temperature, contrary to their prediction.

In terms of the two-state model (eq 5), the decreasing trend in g with increasing temperature is due to the shift in equilibrium from state A toward a less polar state B. That is, $g_B < g_A$. Accordingly, Figure 1 shows a plot of $g - 1$ vs. α as the temperature changes from 0 to 83 °C. The error bars indicate statistical errors within the given theoretical framework. The intercepts define $g_A - 1$ as 2.01 ± 0.12 and $g_B - 1$ as 0.91 ± 0.18.

In spite of the 10–20% statistical uncertainties, the values obtained for $g_A - 1$ and $g_B - 1$, when combined with the respective coordination numbers, go a long way toward defining the structures of the two solvent networks. As a first step, it will be shown that the set (m_A, g_A) defines a flexible tetrahedral network environment. The calculation closely follows the method developed by OK[25a] but adds dipole correlations of higher order than those with nearest neighbors. It also defines the mathematical operation implied by the term "network flexibility" for subsequent use in the interpretation of (m_B, g_B).

To account for network flexibility, one assumes that nearest-neighbor dipoles, in the ensemble average, lose all correlation normal to the O–H··O axis joining them to the central water molecule, as if the molecules were free to rotate about the hydrogen bond (Figure 2a).[28] On the other hand, the component parallel to the O–H··O axis remains correlated. According to eq 4, the contribution to $g_A - 1$ due to four nearest neighbors is then $4 \cos^2(\theta/2)$. One may assume that dipole correlation will be less for next-nearest neighbors and will attenuate rapidly for higher order neighbors. A constant attenuation factor of β per shell will be assumed. The total contribution from all shells then is given in (6).

(27) (a) Grunwald, E. *J. Am. Chem. Soc.* **1984**, *106*, 5414. Correction: *Ibid.* **1986**, *108*, 1361. (b) Grunwald, E. *Progr. Phys. Org. Chem.* **1965**, *3*, 317.

(28) This need not be a continuous rotation. It may be a statistical series of oscillations in the transverse plane such that the ensemble average of the transverse component of the dipole moment is zero.

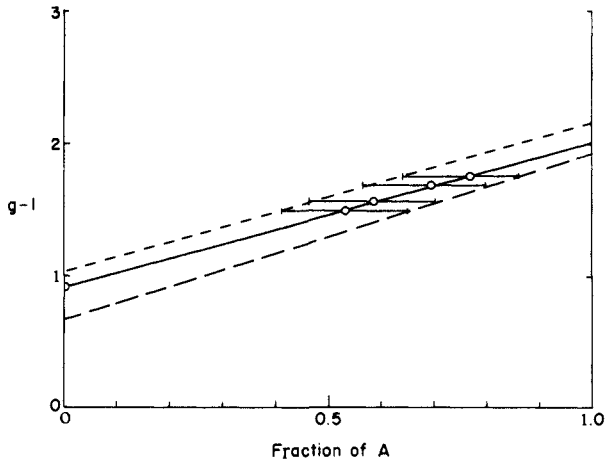

Figure 1. Two-state analysis of Kirkwood correlation factors for water. Solid line, $g - 1$ vs. α. Dashed lines, $g - 1$ vs. $[\alpha \pm \text{ERROR}(\alpha)]$.

$$g_A - 1 = 4\cos^2(\theta/2)(1 + \beta + \beta^2 + \ldots) \quad (6a)$$

$$= 4\cos^2(\theta/2)/(1 - \beta) \quad (6b)$$

To obtain β it is convenient to calculate it first for the assumed tetrahedral configuration of state A and then allow for the statistical distribution of network sites between states A and B by multiplying by $(g - 1)/(g_A - 1)$. The geometry of correlation is shown in Figure 2b. The three next-nearest dipoles add up to a correlated resultant of cos $(\theta/2)$ relative to the nearest neighbor. This resultant rotates as the nearest-neighbor dipole rotates relative to the central water molecule. Its component along the O–H··O axis, which remains correlated to the central water molecule, is $^1/_3$. Thus the ratio (β) of next-nearest- to nearest-neighbor correlation is (7), and g_A is given by (8). In principle, g_A depends

$$\beta = (g - 1)/3(g_A - 1) \quad (7)$$

$$g_A - 1 = \frac{4\cos^2(\theta/2)}{1 - (g - 1)/3(g_A - 1)} \quad (8)$$

on T through the temperature-dependent variable g, but the variation is small enough to be neglected. Plausible values for θ range from 105°, the HOH bond angle chosen by OK,[25a] to 109° 28′, the normal tetrahedral angle. On introducing numerical values for g_A and g (25 °C, Table I), one obtains $\theta = 106°$, which is in the plausible range. The four-coordinated, essentially tetrahedral, network structure derived for state A is shown in Figure 3a.

Five-Coordinated Network Structures. The possible structures are limited by requirements of symmetry, stoichiometry, and flexibility. Symmetry enters as a result of the ergodic theorem: The ensemble average of $\langle\mu_{nwrk}\rangle$ obtained via eq 3 equals the time average of $\langle\mu_{nwrk}\rangle$ for the water shell around a single water molecule. Given enough time, liquids yield to shearing stresses. Therefore, in the time average, the symmetry of the network around a water molecule cannot be lower than the C_{2v} symmetry of the central water molecule's field of force.

Stoichiometry enters because the numbers of hydrogen-bond donor and acceptor sites in the liquid must be equal. This requirement is satisfied by each four-coordinated water molecule with two donor sites and two acceptor sites. As a result, the five-coordinated molecules in the pure liquid must satisfy it independently as a group. Thus there must be two substates at equal concentration: one in which the central molecule is hydrogen bonded to three donors and two acceptors, the other in which there are two donors and three acceptors. Since the water molecule has only two protons, the three hydrogen-donor bonds will be bifurcated hydrogen bonds.

Network flexibility involves the relative motions of connected molecules. It enters as a constraint on network structure because the relative motions in state A must be consistent with those in state B. In the model used for state A, flexibility was treated as

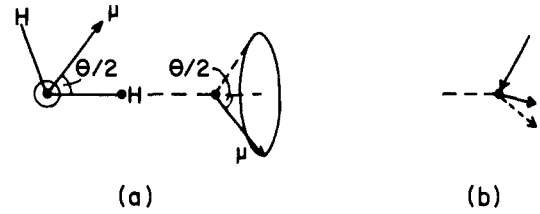

Figure 2. Vector diagrams used in the interpretation of $g_A - 1$. (a) Nearest neighbor, showing flexibility of hydrogen bond. (b) Resultant dipole due to next-nearest neighbors in correlation with nearest-neighbor dipole.

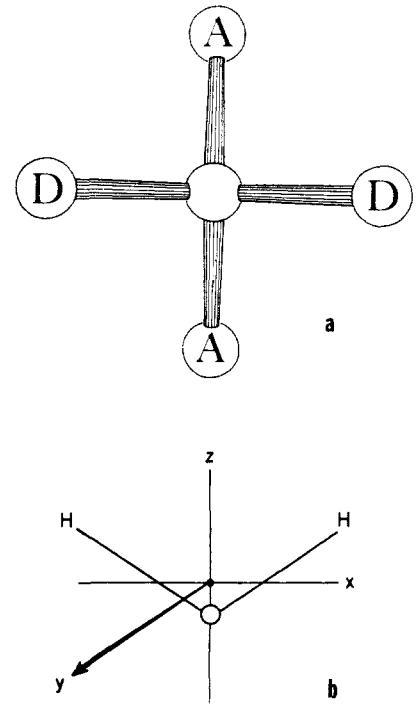

Figure 3. (a) Drawing of nearest-neighbor network structure for four-coordinated state A: (D) H-bond donors; (A) H-bond acceptors. (b) Labeling of Cartesian axes in water molecule.

a localized motion for each hydrogen bond whose effect is equivalent to free rotation about the hydrogen-bond axis.[28] Flexibility of the hydrogen bonds in state B should be defined in the same way.

In addition to satisfying the above constraints, the two five-coordinated network structures must, on average as a pair, agree with the experimental value deduced for $g_B - 1$. Subsequent analysis, especially of the dielectric relaxation data, will suggest, however, that the two *individual* values are nearly equal. This suggestion can be made plausible by a symmetry argument.

In Figure 3b, the only plane which is not a plane of symmetry, and which thus divides the water molecule into two dissimilar halves, is the xy plane. Accordingly, the time-average nearest-neighbor shell around a water molecule may consist of two dissimilar halves. Either half may be polar or nonpolar, subject to the stated constraints. If the number of possible configurations were small, $\langle\mu_{nwrk}\rangle$ would decrease approximately in quanta of one-half. By this argument, it is *not* a coincidence that the five-coordinated state B, with $g_B - 1 = 0.91$, is nearly half as polar as state A: $(g_B - 1)/(g_A - 1) = 0.45$. Both substates of state B apparently have a polar network on one side, and a nonpolar network on the other side, of the xy plane.

Figure 4 shows two five-coordinated network structures favored by the author. In the square pyramid a, the central molecule accepts three hydrogen bonds and donates two. Its protons are directed toward opposite corners of the square. All hydrogen-bonded O–H··O distances are 2.9 Å. The O–O distance along the sides of the square is 3.7 Å, as suggested by the radial dis-

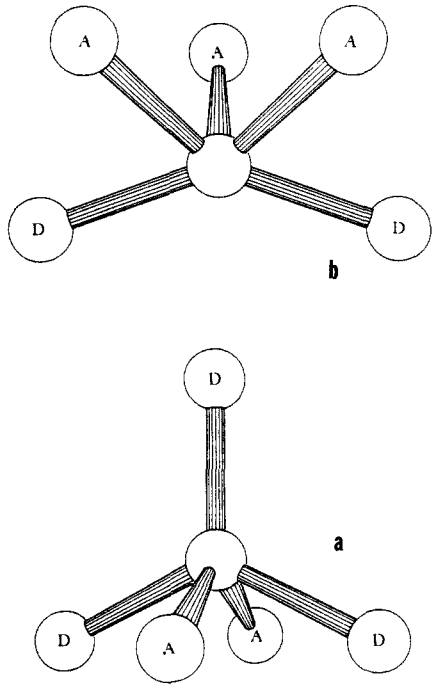

Figure 4. Drawing of nearest-neighbor network structure for complementary five-coordinated network states: (D) H-bond donors; (A) H-bond acceptors.

tribution function. The O–O–O angle at the central molecule toward opposite corners is 127°. Assuming free rotation about each O–H··O axis, the four dipoles of the network molecules in the square give a resultant of zero. The dipole of the apical water molecule in free rotation is $\mu_0 \cos \theta/2$ and is parallel to the dipole of the central molecule. Hence $\mu_{nwrk} = (\mu_0 \cos \theta/2)/(1 - \beta)$, and when $\theta = 109°\ 28'$, $(g_B - 1)/(g_A - 1) = 0.43$.

In structure b of Figure 4, the central molecule accepts two hydrogen bonds at the normal tetrahedral acceptor sites. These molecules are regarded as rotating freely and contribute $2\mu_0 \cos^2 (\theta/2)/(1 - \beta)$ to μ_{nwrk}. The three network molecules on the opposite side of the xy plane are bound by bifurcated hydrogen bonds to the two protons of the central molecule in the isosceles array of a symmetric top. Their ensemble-average dipoles face outward, with three-fold symmetry, nearly parallel to the xy plane, so that their contribution to μ_{nwrk} is nearly zero. Accordingly, $(g_B - 1)/(g_A - 1)$ is nearly $^1/_2$. The three molecules that are bound by bifurcated hydrogen bonds thus are not free to rotate about the O–O axis joining them to the central molecule. They retain significant flexibility, however, by being able to rotate about and to rock in any direction normal to their own z axis. The fraction of such bifurcated hydrogen bonds in the overall liquid is $(3/10)(1 - \alpha)$ and ranges from 0.07 at 0 °C to 0.14 at 83 °C. It is small enough for the disparity in flexibility to be neglected in first approximation, but the mere fact that two kinds of flexibility seem to be required precludes the two-state model from being exact.

Molar Volume. By simply counting the central water molecule and its nearest neighbors, the volume occupied by five molecules in state A is nearly equal to that occupied by six molecules in state B. The molar volumes, which vary inversely as the molecular densities of the states, are therefore in the ratio $v_A/v_B \simeq {}^6/_5$. Adopting an icelike value of 20 mL/mol for v_A, one predicts that $\Delta v_{A,B} \simeq -3.3$ mL/mol.

The preceding estimate based on molecular densities may be compared with other estimates of $\Delta v_{A,B}$. Benson[9] estimates from thermodynamic data that $\Delta v_{A,B} = -3.2$ mL/mol. The effect of pressure on ultrasonic relaxation, when interpreted in terms of a two-state model, leads to $\Delta v_{A,B} = -4$ mL/mol.[17b] Other estimates, reviewed by Davis and Jarzynski,[12a] range from −3 to −7 mL/mol.

Potential Energy. The remainder of this paper will consider whether the electrostatic network properties expressed by g_A and

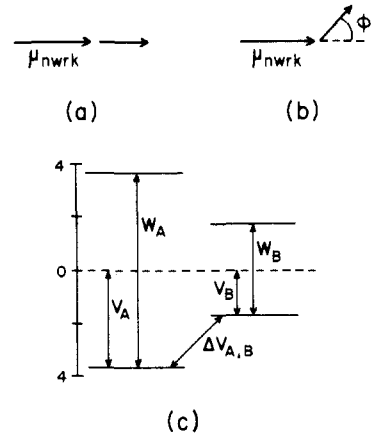

Figure 5. Dipole–dipole model for hindered rotation. (a) Potential minimum. (b) Rotation of the central water molecule relative to its network. (c) Energy level diagram.

g_B are consistent with thermodynamic properties, as expressed by $\Delta H_{A,B}$ and $\Delta S_{A,B}$, with intermolecular vibration frequencies, and with kinetics and mechanism in dielectric relaxation. As a first step, we shall derive an expression for the electrostatic interaction energy between the central water molecule and the surrounding network in its time-average configuration. This derivation is similar, conceptually, to the Kirkwood–Westheimer calculation of interaction energies among electrostatic poles imbedded in organic molecules.[29] The water molecules are treated as point dipoles. The medium in which the dipoles interact is treated as a dielectric continuum whose polarization is entirely due to distortion polarization. The effective dielectric constant for the interaction therefore is n^2, where n denotes the optical refractive index.

Accordingly, the pairwise interaction energy $V_{0,i}$ between the central dipole μ_0 and the ith dipole in its solvent network is expressed by eq 9, where r_{0i} is the distance or vector displacement between the dipoles.[30]

$$V_{0i} = \frac{\mu_0 \cdot \mu_i}{n^2 r_{0i}^3} - \frac{3(\mu_0 \cdot r_{0i})(\mu_i \cdot r_{0i})}{n^2 r_{0i}^5} \tag{9}$$

Equation 9 can be simplified because the calculation is for the solvent network in its time-average configuration. Instead of using instantaneous dipole vectors, one may therefore use ensemble averages such as $\langle \mu \rangle_i$ for the ith nearest neighbor or $\langle \mu' \rangle_i$ for the higher-order neighbors correlated with the ith neighbor. Owing to the flexibility of the hydrogen bonds, these ensemble-average dipoles are directed along the O–H··O hydrogen bond axis to the central water molecule. Thus, for the nearest neighbor, $\langle \mu \rangle_i$ and r_{0i} are parallel vectors. For the group of next-nearest-neighbor molecules hydrogen bonded to that nearest neighbor, the resultant group dipole $\langle \mu' \rangle_i$ is parallel to $\langle \mu \rangle_i$, and the displacement vector r'_{0i} to the centroid of the group is practically parallel to $r_{0,i}$. For higher order neighbor shells the parallel model becomes less accurate, but such shells make only a small contribution to the total interaction energy.

Because the vectors $\langle \mu \rangle_i$ and r_{0i} to nearest neighbors are parallel, and those to higher order shells are nearly so, there are several consequences. First, for the ith nearest neighbor, eq 9 simplifies to (10). Second, for the entire solvent network, neglecting de-

$$V_{0i} = -2\mu_0 \cdot \langle \mu \rangle_i / n^2 r_{0i}^3 \tag{10}$$

$$V = -2\mu_0 \cdot \Sigma [\langle \mu \rangle_j / n^2 r_{0j}^3] \tag{11}$$

viations from parallelism for higher order shells, superposition of terms of the form (10) leads simply to (11). The summation in

(29) (a) Kirkwood, J. G.; Westheimer, F. H. *J. Chem. Phys.* **1938**, *6*, 506. (b) Westheimer, F. H.; Kirkwood, J. G. *J. Chem. Phys.* **1938**, *6*, 513; *Trans. Faraday Soc.* **1947**, *43*, 77.

(30) Boettcher, C. F. J.; Van Belle, O. C.; Bordewijk, P.; Rip, A. *Theory of Electric Polarization*, revised ed.; Elsevier: Amsterdam, 1973; Vol. 1, Chapter 3.

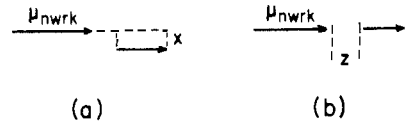

Figure 6. Dipole–dipole model of libration. Straight-line displacement without rotation: (a) along x and y; (b) along z.

(11) extends over all nearest neighbors and over the next-nearest and higher order shells hydrogen-bonded to them. Equation 11 can be further simplified by defining an energy-weighted average dipole–dipole distance r_p according to (12). Substitution in (11)

$$\mu_0 \cdot \sum[\langle \mu_j \rangle / r_{0j}^3] = [\sum \mu_0 \cdot \langle \mu \rangle_j] / r_p^3 = \mu_0 \cdot \langle \mu_{nwrk} \rangle / r_p^3 \quad (12)$$

$$V = -2\mu_0 \cdot \langle \mu_{nwrk} \rangle / n^2 r_p^3 \quad (13)$$

$$V = -2\mu_0^2 (g - 1) / n^2 r_p^3 \quad (14)$$

then yields (13), and application of (4) yields (14), which expresses the desired connection between the time-average electrostatic interaction energy and the ensemble-average dipole correlation in the surrounding network. To evaluate r_p we shall apply Eq. 6a. Accordingly, a fraction $(1 - \beta)$ of $\langle \mu_{nwrk} \rangle$ is due to nearest-neighbor sites at 2.9 Å. The remaining fraction β will be placed at the next-nearest-neighbor distance of 4.8 Å. On solving for β according to (7) one finds that $r_p = 3.15$ Å.

The time-average interaction energy of the central water molecule with its solvent network in state A or B is obtained directly from (14) by letting $g = g_A$ or g_B, respectively. $\mu_0 = 1.88$ D, $n = 1.333$, $r_p = 3.15$ Å^0, and g values are taken from Table I. Results are as follows: $g = g_A$; $V_A = -3.68$ kcal/mol. $g = g_B$; $V_B = -1.66$ kcal/mol. $\Delta V_{A,B} = 2.02$ kcal/mol. The value obtained for $\Delta V_{A,B}$ is similar to the 2.5 kcal/mol given previously for $\Delta H_{A,B}$.

To derive the barrier to rotation of the central water molecule, we note that in the ensemble average, μ_0 and $\langle \mu_{nwrk} \rangle$ are aligned head to tail (Figure 5a). We then allow the central water molecule to rotate about an axis in the xy plane (Figure 3b) while $\langle \mu_{nwrk} \rangle$ remains stationary (Figure 5b). The interaction energy, according to (13), is now given by (15), The following results

$$V(\phi) = (W/2) \cos \phi \quad (15a)$$

$$W = 4\mu_0^2 (g - 1) / n^2 r_p^3 \quad (15b)$$

are obtained for states A and B: state A, $g = g_A$, $W_A = 7.36$ kcal/mol; state B, $g = g_B$, $W_B = 3.33$ kcal/mol. A potential energy diagram comparing V_A and W_A with V_B and W_B is given in Figure 5c.

Equations 13–15 are remarkable for their formal simplicity, and since they will prove useful and fairly accurate, we shall consider briefly what happened to the individual hydrogen-bond energies.

As is well-known, the hydrogen bonds in water leave their mark on many properties. For example, proton delocalization resulting from hydrogen-bond formation leads to ultrafast proton transfer.[27b] However, in theoretical calculations of hydrogen-bond energies, electron and proton delocalization are often neglected and a classical electrostatic approach is sufficient. Such an approach is adopted, for example, in some of the recent computer simulations of liquid water.[4a] It is also adopted here, and leads to the following notable result for the time-average configurations. Even though all hydrogen bonds are counted, the dipole–dipole energy for the central water molecule is proportional to $g_A - 1$ or $g_B - 1$ rather than to the number of hydrogen bonds to nearest neighbors, because of geometrical factors. In particular, in state B some of the dipoles oppose each other. As a result, within this theoretical framework, the energy per hydrogen bond is *not* constant.

The expressions for the potential energy of a water molecule interacting with its time-average network environment obtained in this section will now be used in a quantum-mechanical calculation of energy levels for a water molecule in its network environment and then of $\Delta S_{A,B}$ and $\Delta H_{A,B}$.

$\Delta H_{A,B}$, $\Delta S_{A,B}$, and $\Delta G_{A,B}$. The internal motions of a water molecule are nearly the same in states A and B.[9,17a] The motions which depend on the network environment are the six modes that can be correlated with rotation and translation in the gas phase. According to the preceding dipole model, rotation about the dipole (z axis, Figure 3b) remains free, but rotation about an axis in the xy plane is hindered by the barrier W_A or W_B. While the barrier is characteristic of the state, the reduced moment of inertia I for rotation of the water molecule relative to the surrounding network is not: $I = I_{HOH} I_{nwrk} / (I_{HOH} + I_{nwrk}) \simeq I_{HOH}$, because I_{nwrk} is large.

Table II. Further Data for Two-State Model of Water

moments of inertia, g cm^2 × 10^{40} [a]	
I_x	1.002
I_y	2.947
I_z	1.921
barriers, kcal/mol[b]	
W_A	7.36
W_B	3.33
hindered rotation; oscillator frequency, s^{-1} [c]	
$\nu_{A,x}$	8.0 × 10^{12}
$\nu_{A,y}$	4.7 × 10^{12}
$\nu_{B,x}$	5.4 × 10^{12}
$\nu_{B,y}$	3.2 × 10^{12}
libration; oscillator frequency, s^{-1} [d]	
$\nu_{A,x}$, $\nu_{A,y}$	1.6 × 10^{12}
$\nu_{B,x}$, $\nu_{B,y}$	7.3 × 10^{11}
$\Delta S_{A,B}$, cal/(mol K)	
hindered rotation	1.94
libration	2.36
mixing, state B	1.38
total	5.68

[a] From infrared spectrum of vapor. [b] Equation 14. [c] $(W/2I)^{1/2}/2\pi$. [d] $[3\mu^2(g-1)/(n^2\pi^2 r_p^5 m_{HOH})]^{1/2}$.

The calculation of thermodynamic properties for hindered rotation is facilitated by the tables of Pitzer and Gwinn.[31] State A with the higher barrier has the wider spacing of energy levels and hence the lower entropy. Near the bottom of the potential well the oscillator frequency ν, included in Table II, is $(W/2I)^{1/2}/2\pi$. From the tables of Pitzer and Gwinn[31] and physical data listed in Table II, $\Delta S_{A,B}$ for the hindered rotations is found to be 1.90 cal/(mol K).

$\Delta S_{A,B}$ for libration (hindered translation) cannot be calculated similarly by an established method, but a reasonable estimate can be made. The librations are straight-line motions without rotation (Figure 6). Near the bottom of the potential well the potential energy is dominated by the dipole–dipole interaction. For small displacements along x and y the dipole–dipole potential is nearly harmonic. The force constant (calculated by a generalized version of eq 9) is $k(g_A - 1)$ in state A and $k(g_B - 1)$ in state B, where $k = 12\mu_0^2 / n^2 r_p^5$. The corresponding oscillator frequencies for libration are included in Table II. They are less than kT/h and vary as $(g - 1)^{1/2}$. At higher energies the potential walls become steeper (model of particle in a box) and the energy levels move further apart. Thus most of the molecular population occupies energy levels whose spacing is proportional to $(g_A - 1)^{1/2}$ and $(g_B - 1)^{1/2}$, respectively. Accordingly, $\Delta S_{A,B}$ for libration along x and y is given approximately by $(R/2) \ln [(g_A - 1)/(g_B - 1)]$ per mode. Libration along z cannot be treated as simply, but it is reasonable to adopt the same approximation. The total for three modes of libration is given in Table II.

Finally, state B is a mixture of two substates of nearly equal g values, with a 3:2 and 2:3 donor:acceptor ratio of hydrogen bonds; see Figure 4. Hence there is an entropy of mixing, which is approximated in Table II by $R \ln 2$. The total $\Delta S_{A,B}$ thus is calculated to be 5.68 cal/(mol K), in fairly good agreement with Benson's value[9] of 6.75 cal/(mol K), which was used as an input value.

$\Delta H_{A,B}$ will be calculated by using the value of $\Delta V_{A,B}$ obtained in the preceding section. The difference involves zero-point energies and thermal energies. The six modes that we are considering are low-frequency modes, with $(h\nu/kT) \leq 1$. For a harmonic

(31) Lewis, G. N.; Randall, M.; Pitzer, K. S.; Brewer, L. *Thermodynamics*, 2nd, ed.; McGraw-Hill: New York, 1961; Chapter 27.

oscillator, when $(h\nu/kT) \leq 1$, $H - V = RT[1 + 0.083 \times \mathrm{ORDER}(h\nu/kT)^2] \simeq RT$ per mol. Accordingly, $\Delta H_{A,B} \simeq \Delta V_{A,B} = 2.02$ kcal/mol, comparable with Benson's value[9] of 2.5_1 kcal/mol which was used as an input value.

$\Delta G_{A,B} = \Delta H_{A,B} - T\Delta S_{A,B}$. At 298 K the value is 0.33 kcal/mol by the dipole–dipole model, comparable with Benson's value[9] of 0.50 kcal/mol.

Values of α_{dip} based on the dipole–dipole model are included in Table I. The values are given in parentheses because the calculation is not self-consistent—the input values are listed in the α column. However, the discrepancies are fairly small, and one is tempted to conclude that the dipole–dipole potential used does not significantly degrade the approximation inherent in the original two-state model for liquid water.

Frequencies for Libration and Hindered Rotation. Experimental Raman, infrared, and inelastic neutron scattering spectral frequencies assigned to intermolecular vibrations in liquid water have been summarized by Walrafen.[13b] The two lowest frequency spectral bands are centered at $(1.6–1.8) \times 10^{12}$ and $(4.8–5.1) \times 10^{12}$ s^{-1}, respectively. By comparison, the frequencies predicted in the preceding section (Table II) give the following state-fraction averages: $1.3_4 \times 10^{12}$ s^{-1} for libration and $5.7_4 \times 10^{12}$ s^{-1} for hindered rotation. Although the state-fraction averages make no allowance for probable differences in transition probabilities, the agreement with experiment is clearly better than merely qualitative. To the best of the author's knowledge, this is the first model prediction of frequencies for libration and hindered rotation in the water network which comes close to reproducing experimental results.

Dielectric Relaxation. In principle, barriers to rotation can be deduced from dielectric relaxation. It will now be shown that the dielectric relaxation spectrum of water, which has been carefully reviewed by Hasted,[32] confirms W_B, the smaller of the two barriers.

The relaxation spectrum shows two well-resolved steps: The slower step, with $\tau = 9.3$ ps at 20 °C, lowers the dielectric constant from its static value near 80 to about 4.3. Although the frequency dependence in this step deviates somewhat from that for a pure Debye relaxation, as is normal for a liquid, the implied distribution of relaxation times is uncommonly narrow.[32]

The faster step in the relaxation spectrum, with $\tau = 0.25$ ps, lies in the far-infrared. It is indistinct and hard to characterize, partly because this spectral region also contains resonant absorptions.[32]

The relaxation spectrum raises several questions, chief among them: Why are there two steps rather than only one? For large polar molecules two or more steps are common. One step is assigned to rotation of the molecule as a whole and the others to independent rotation of flexible polar part-structures. In case of a small molecule like water, however, one can have only rotation of the entire molecule. For definiteness, consider two states of water molecules, A and B. One may then write eq 16 for the total

$$\frac{1}{\tau} = \frac{\alpha}{\tau_A} + \frac{(1-\alpha)}{\tau_B} \qquad (16)$$

rate of relaxation. Although (16) shows two relaxation times, τ_A and τ_B, one observes only the single relaxation time τ if the transfer of polarization between states A and B is so fast that the two states remain essentially at polarization equilibrium throughout the relaxation process. This is probably the case. Electric fields, and hence the torques acting on a dipole, travel with the speed of light and thus reach a neighboring molecule in 10^{-18} s. Inequalities of polarization then relax in the time during which the molecules undergo hindered rotation in their potential wells, ca. 0.2 ps. (See preceding section.) Indeed, according to the mechanism to be described, the transfer of polarization occurs with a relaxation time equal to τ for the faster step, in ca. 0.25 ps, and thus is 1–2 orders of magnitude faster than the slower step.

Table III. Test of Eq 22

T, °C	ϵ_∞[32]	$10^{24}\chi_{or}$, cm^3 from ϵ_∞	$10^{24}\chi_{or}$, cm^3 calcd, eq 22
0	4.46	4.6	3.4
10	4.10	4.0	3.8
20	4.23	4.2	4.2
30	4.20	4.2	4.7
40	4.16	4.2	5.1
50	4.13	4.1	5.5
60	4.21	4.3	6.0
75	4.49	4.8	6.5
		av 4.3	4.9

In the following, $1/\tau$ for the slower step will be analyzed according to eq 16. Rotation about the z axis does not change the dipole vector, and this degree of freedom therefore is not affected by an electric field. The analysis accordingly is limited to rotation about any axis in the xy plane of the water molecule. For molecules in a given state, according to the dipole model, the barrier is independent of the direction of the axis of rotation in that plane. However, W_A is greater than W_B by 4 kcal. (An energy level diagram is given in Figure 5c.) Even after allowing for a difference in $\Delta S^\ddagger$, α/τ_A will be less than 5% of $(1-\alpha)/\tau_B$ at temperatures of interest and hence may be neglected in eq 16.

From average values for $1/\tau$ given in Hasted's review and $(1-\alpha)$ based on the input data from Benson's analysis (Table I), the theoretically predicted values of $1/\tau_B$ are reproduced by eq 17 in the temperature range 0–50 °C with a mean deviation of

$$1/\tau(1-\alpha) = 1/\tau_B = (4.8 \pm 1.0) \times 10^{13} \exp[(-1434 \pm 60)/T] \qquad (17)$$

only 2.4%. (There may be a little curvature.) To obtain W_B, one expresses $1/\tau_B$ similarly in terms of $\Delta H_B^\ddagger$ and a preexponential factor A_B, as in (18). The exponential term in (17) then gives

$$1/\tau_B = A_B \exp(-\Delta H_B^\ddagger/RT) \qquad (18)$$

$\Delta H_B^\ddagger = 2.85$ kcal/mol. After applying a small correction for zero-point and thermal energy, $W_B = 3.07 \pm 0.15$ kcal/mol, practically equal to the value of 3.33 ± 0.6 kcal/mol computed from $(g_B - 1)$.

The preexponential factor A_B is also of the correct magnitude for the assumed mechanism. According to transition state theory,[33] rate constants for rotation are given by (19), where Ω_+ is the mean

$$k_+ = \Omega_+ K_+^\ddagger = \Omega_+ \exp(\Delta S^\ddagger/R) \exp(-\Delta H^\ddagger/RT) \qquad (19)$$

angular velocity across the barrier in the forward direction. To obtain an expression for dielectric relaxation, note that (a) $1/\tau = k_+ + k_-$, (b) $K_+^\ddagger = K_-^\ddagger$, and (c) $\Omega_+ = \Omega_-$. Furthermore, Ω_+ consists of kinetically parallel processes of rotation about x and y: $\Omega_+ = \Omega_x + \Omega_y$. Furthermore, there is a geometric factor of $^1/_3$ because the electric field is polarized in one direction. The result is (20). Calculation for a rotor with barrier W_B and

$$1/\tau = (2/3)(\Omega_x + \Omega_y) \exp(\Delta S^\ddagger/R) \exp(-\Delta H^\ddagger/RT) \qquad (20)$$

moments of inertia I_x and I_y indicates that $0.7 < \exp(\Delta S^\ddagger/R) < 1.4$. Hence the preexponential factor in (17) should be close to $(2/3)(\Omega_x + \Omega_y)$. If one adopts a model of classical rotation, $\Omega_{x,y} = (2\mathrm{KE}/I_{x,y})^{1/2}$. Letting KE, the rotational kinetic energy, equal $W_B/2$ + (mean energy above barrier), one obtains $(2/3)(\Omega_x + \Omega_y) = 5.1 \times 10^{13}$, compared to the factor 4.8×10^{13} in eq 17. The near identity of the numbers may be fortuitous, but the agreement is clearly good.

It remains to show that the faster step in the relaxation spectrum is not a spoiler—that it can be interpreted by a compatible mechanism. This is necessary because, at the time of Hasted's review,[32] it was not possible to fit a mechanism. To do so, the author will risk extrapolating the previously used two-state model to frequencies near 300 GHZ. This is a risk because the network

(32) Hasted, J. B. In *Water, A Comprehensive Treatise*; Franks, F., Ed.; Plenum Press: New York, 1972; Vol. 1, Chapter 7.

(33) See, for example: Hammett, L. P. *Physical Organic Chemistry*, 2nd ed; McGraw-Hill: New York, 1970; Chapter 5.

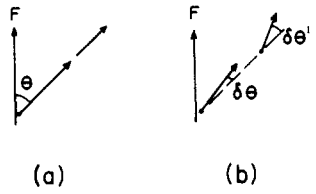

Figure 7. Model used in calculation of χ_{or}. (a) The dipoles are oriented in the direction of the unperturbed minimum. (b) Potential minimum in the presence of the internal field F.

properties to be used are those for the time-average configuration and thus apply only if the period of observation (ca. one cycle of the alternating field) is long compared to periods for libration and hindered rotation of a water molecule in its network. Judging by the frequencies in Table II, at 300 GHz this requirement is on the verge of not being satisfied.

The property to be analyzed is the dielectric constant at the beginning of the faster step, which is expressed by ϵ_∞ for the slower step and is measured at about 300 GHz. Values at various temperatures are listed in Table III. All are significantly greater than the value of $n^2 = 1.8$ expected for distortion polarization alone.

The gist of the mechanism to be proposed is that at frequencies at which the slower step is unable to follow, one can still have orientation polarization because the electric field perturbs eq 15 and produces a small change in the angle ϕ at which $V(\phi)$ is at a minimum. This in turn slightly polarizes the molecular population in the potential well. Debye has shown that when the unperturbed well is symmetric, such polarization is independent of the temperature.[34] In terms of eq 3, it contributes an additive term to the polarizability: $\chi = \chi_{distortion} + \chi_{or}$.

Table III lists values of χ_{or} calculated from ϵ_∞ via eq 3 by letting $g\mu^2/3kT = 0$ and $\chi_{distortion} = 1.5 \times 10^{-24}$, the value used by OK.[22] In Figure 7, let θ denote the angle between the internal field F and the dipole direction in the unperturbed minimum. Let $\delta\theta$ and $\delta\theta'$ denote respectively the deviations of μ and μ_{nwrk} from θ. The perturbed potential minimum then is located according to (21).

$$\delta\theta = -2a(1 - g/3) \qquad \delta\theta' = 2a(1 - 2g/3)$$
$$a = 2\mu F(\sin\theta)/W \tag{21}$$

The moment m induced in the central water molecule is $-\mu\delta\theta \sin\theta = 4\mu^2 F(\sin^2\theta)(1 - g/3)/W$. The mean induced moment $\langle m \rangle$ is then obtained by averaging m over all possible directions. The resulting polarizability is $\langle m \rangle/F$.

$$\chi_{or} = \langle m \rangle/F = \int_0^\pi (m(\sin\theta)/2F)\, d\theta$$
$$= 8\mu^2(1 - g/3)/3W \tag{22}$$

Application of the two-state model then gives (23). Because 1

$$\chi_{or} = \frac{8\mu^2}{3}\left[\frac{\alpha(1 - g_A/3)}{W_A} + \frac{(1 - \alpha)(1 - g_B/3)}{W_B}\right] \tag{23}$$

$- g_A/3 \simeq 0$, χ_{or} depends practically on state B. Equation 23 involves no new parameters.

Values calculated from (23) are included in Table III. They are clearly of the correct magnitude; the averages for the columns based on ϵ_∞ and on eq 23 agree within the error limits. On the other hand, the values predicted from (23) show the greater temperature coefficient. On the whole, the agreement is good enough to warrant refinement of the model to allow for the high spectral frequency.

Concluding Remarks. By defining the two states as water molecules with two different coordination numbers in a flexible network, some of the theoretical misgivings about the two-state model of water may have been overcome. If the two-state model is accepted, then the second, five-coordinated state is now as well characterized as the familiar four-coordinated state of Bernal and Fowler[22] has been for some time. In its proposed version, the two-state model also explains some of the apparent "schizophrenia" of water. While some properties (such as the oxygen–oxygen radial distribution function of Morgan and Warren[24a]) are dominated by features ascribable to the four-coordinated state, others (such as the dielectric relaxation spectrum) do not fit such a model at all, being dominated by the five-coordinated state. In its proposed version, the two-state model in no way forbids appropriate infrared spectral properties from reflecting quasi-continuous microscopic distributions and, thus, may defuse a controversy of long standing.[17a] Discreteness of state properties is expected only if the time scale of the experiment is long enough (probably at least 1 ps) to sample the time-average state of the network, and this is clearly not true at infrared frequencies. Finally, the mixing of four-coordinated and five-coordinated states results in a network with long-range disorder and thus satisfies an essential theoretical requirement for a liquid.

Registry No. H_2O, 7732-18-5.

(34) Debye, P. *Polar Molecules*, Dover Publications: New York, 1945; p 21.

Thermodynamic Properties of Nonpolar Solutes in Water and the Structure of Hydrophobic Hydration Shells[1]

Ernest Grunwald

Contribution from the Chemistry Department, Brandeis University, Waltham, Massachusetts 02254. *Received February 14, 1986*

Abstract: Experimental partial molar entropies and heat capacities in water for noble gases, nonpolar diatomic gases, and hydrocarbons were analyzed thermodynamically by delphic dissection to evaluate the contributions from solute-induced perturbations of the water network. These contributions, which are typically large, were then interpreted in terms of the familiar two-state model of liquid water. Changes in the fractions of the two states and of their relative enthalpies, per mole of solute, were thus evaluated. The numbers of water molecules that are nearest neighbors to the solute, and the manner in which the nearest neighbors are tied to the bulk water network, could be elucidated.

Liquids, like crystals, are conveniently classified into molecular and network categories. Water, with its hydrogen-bonded structure,[2,3] is a network liquid. Solvation of a nonelectrolyte solute in a network liquid consists of two parts. There is ordinary direct

0002-7863/86/1508-5726$01.50/0